Studies of Plastic-Ablator Compressibility for Direct-Drive Inertial Confinement Fusion on OMEGA

S. X. Hu,* V. A. Smalyuk, V. N. Goncharov, J. P. Knauer, P. B. Radha, I. V. Igumenshchev, J. A. Marozas, C. Stoeckl, B. Yaakobi, D. Shvarts,† T. C. Sangster, P. W. McKenty, D. D. Meyerhofer,‡ S. Skupsky, and R. L. McCrory‡

Laboratory for Laser Energetics, University of Rochester, 250 East River Road, Rochester, New York 14623-1299, USA

(Received 7 December 2007; published 6 May 2008)

The compression of planar plastic targets was studied with x-ray radiography in the range of laser intensities of $I \sim 0.5$ to 1.5×10^{15} W/cm^2 using square (low-compression) and shaped (high-compression) pulses. Two-dimensional simulations with the radiative hydrocode DRACO show good agreement with measurements at laser intensities up to $I \sim 10^{15}$ W/cm^2. These results provide the first experimental evidence for low-entropy, adiabatic compression of plastic shells in the laser intensity regime relevant to direct-drive inertial confinement fusion. A density reduction near the end of the drive at a high intensity of $I \sim 1.5 \times 10^{15}$ W/cm^2 has been correlated with the hard x-ray signal caused by hot electrons from two-plasmon-decay instability.

DOI: 10.1103/PhysRevLett.100.185003 PACS numbers: 52.57.−z, 51.35.+a, 52.65.−y

Understanding the compressibility of ignition-relevant ablator materials is crucial for inertial confinement fusion (ICF) target designs [1,2]. In direct-drive ICF, a spherical shell consisting of a thin outer plastic ablator and thick inner cryogenic DT fuel is uniformly driven by overlapping laser beams [3]. Ignition has been predicted when the shell is compressed ~1000 times and the burn wave propagates from the central hot spot to the outer shell [3]. To achieve such high compression, the target has to be driven with high energy [e.g., the National Ignition Facility (NIF) [4]], of ~1-MJ low adiabat ($\alpha \approx 2$, defined as the ratio of shell pressure to the Fermi-degenerate pressure) pulses that send precisely timed shock and compression waves through the fuel to achieve required compression. Measuring the density profiles of laser-driven targets and comparing them to code predictions are essential to understand laser-compression physics for ICF [3]. A variety of techniques have been applied to diagnose density and temperature conditions of laser-driven targets. For example, absorption spectroscopy in aluminum layers was used to infer the temperature of shock-heated ablators [5–7]. X-ray scattering has provided information on shell conditions [8–10]. Direct measurements of the density profiles of laser-driven polystyrene ablators at relatively low intensity ($\sim 7 \times 10^{13}$ W/cm^2) have been made [11–13], in which a peak density of 2–3 g/cm^3 was inferred. Shock compression of D_2 and other materials have also been investigated at pressures less than ~10 Mbar [14–19]. For ignition-relevant laser intensities (ablation pressure greater than ~50 Mbar), direct measurements and comparisons with code predictions for large compressions of laser-driven ablator materials have not been previously presented. These measurements can be used to validate some aspects of ablator-compression physics such as the equation-of-state and shock-wave dynamics implemented in the ignition-design codes [20]. This Letter presents the first experimental results and comparisons to code predictions on plastic-ablator compression in the laser intensity range from $I \sim 0.5$ to 1.5×10^{15} W/cm^2. (Note that the baseline direct-drive target design has a peak intensity of 10^{15} W/cm^2). Our results provide the first experimental evidence for low-entropy, adiabatic compression of plastic shells in the laser intensity regime relevant to direct-drive ICF.

In the experiments described in this Letter, plastic targets with a thickness of ~125 μm, length of ~2 mm, and a width of ~280 μm were irradiated by 351-nm laser light at peak intensities varying from ~0.5 to 1.5×10^{15} W/cm^2, using both square and shaped pulses on the OMEGA Laser System [21]. A schematic of the experiment setup is shown in Fig. 1, in which 14 overlapped beams drive the target. The beam configuration included two beams at 10.3° angle of incidence and four beams for each angle of incidence at 31.7°, 42.2°, and 50.5°, respectively. The standard beam-smoothing techniques including distributed phase plates [22], polarization smoothing [23], and smoothing by spectral dispersion [24] were employed. The target compression was measured with x-ray, side-on radiography using ~5.2-keV vanadium (V) or ~6.4-keV

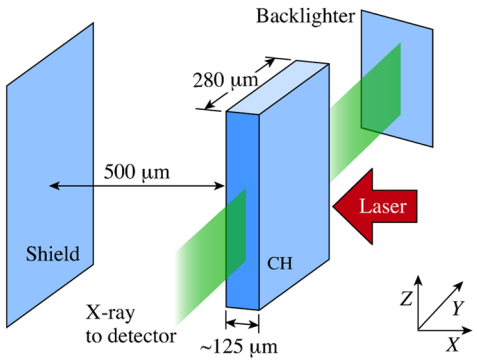

FIG. 1 (color online). The schematic diagram of the compressibility experiment setup.

iron (Fe) backlighters (irradiated by six additional beams.) Since the beam size was larger than the target width, a plastic shield was placed ~500 μm behind the target to intercept laser light missing the target. Target compression was measured with a framing camera that recorded two images on each shot with a temporal resolution of ~40 ps and a spatial resolution of ~8 μm [25]. The uncertainty of absolute timing of framing-camera images with respect to laser drive was ~100 ps, while the uncertainty of timing between images was ~20 ps.

The absorption of backlighter x-ray emission by the compressed target attenuates the x-ray intensity according to $I_x = I_0 e^{-\mu(h\nu)\rho L}$, where $\mu(h\nu)$, ρ, and L are the photon-energy-dependent absorption coefficients, the density, and the target width, respectively. Knowing the target width and the absorption coefficients, one can infer the density of the compressed target from the x-ray-intensity attenuation. The optical depth, which is defined as the natural logarithm of x-ray-intensity attenuation, is used as a measure of the target compression. The two-dimensional (2D) radiative hydrocode DRACO was used to model the detailed experimental configurations. The simulation plane was spanned by the shock propagation direction (x axis) and the target width (y axis). Both the standard constant flux limiter of $f = 0.06$ [26,27] and a nonlocal model [28] were considered for the thermal-transport modeling. Both models give similar predictions for the compression. Their differences cannot be distinguished in the experiments, given the experimental timing uncertainty of ~100 ps and insensitivity to small (~ 10%) density variations. The simulations took into account temporal and spatial resolution of the diagnostics. The measured optical depths were directly compared with the 2D simulations.

Figure 2(a) shows an example of the simulation of a target driven by 1-ns square pulse at a peak intensity of $I \simeq 1.5 \times 10^{15}$ W/cm^2 taken at 0.6 ns. It represents a density profile on the simulated x-y plane (x is the shock propagation axis and y is the target width; see Fig. 1). The front surface is initially at $x = 0$. Figure 2(b) shows the measured image of the target at the same time of $t = 0.6$ ns, formed by x rays traversing the target along the y direction. The absorption image is obtained in the x-z plane, as it was viewed along the y axis (see Fig. 1). The shock, launched by the laser drive, compresses the target as it propagates in the x direction from right to left. If the target is sufficiently wide, the uniform irradiation essentially drives a 1D shock propagation in the target. However, to allow optimum imaging with V and Fe backlighters, the target width was chosen to be slightly smaller than the spot size of the laser beams. As a result, the target sides were irradiated and the plastic shield reflected small amount of lights to the target back surface. This launched a weak shock from the target back surface, counter-propagating toward the main laser-driven shock from the target front surface. The side illuminations generate weak shocks from the target sides causing more compression around the target edges. These detailed

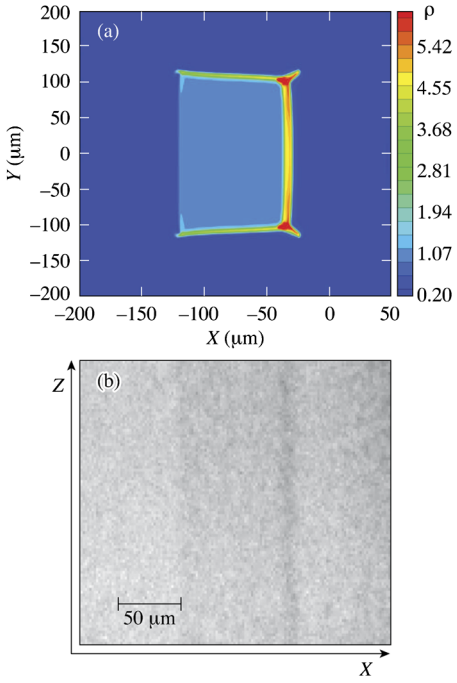

FIG. 2 (color online). (a) The target density profile from the 2D DRACO simulation for a 1-ns square pulse at $t \simeq 0.6$ ns; (b) the corresponding x-ray-absorption imaging from the experiment.

features can be well modeled by the 2D DRACO simulations indicated in Fig. 2(a). The corresponding optical-depth comparison will be shown in Fig. 5(b).

Figure 3 shows experimental results and their comparisons with 2D simulations for a 1.6-ns square pulse [Figs. 3(a)–3(c)] and a 3-ns shaped (low-adiabat) pulse [Figs. 3(d)–3(f)]. The laser drive of the 1.6-ns pulse has a peak intensity of $\sim 5 \times 10^{14}$ W/cm^2 [Fig. 3(a)]. It sends a single shock with a pressure of $p \approx 55$ Mbar that compresses the target to a peak density of $\rho \approx 4.3$ g/cm^3 from the initial density $\rho_0 \approx 1.044$ g/cm^3. The compression is right on the polystyrene (CH) Hugoniot. The target absorption, or optical depth, versus target position X is shown at 0.8 ns [Fig. 3(b)] and at 1.5 ns [Fig. 3(c)], which was measured with a V backlighter. While the shock is traversing the target at 0.8 ns, it reached the back side of the target at 1.3 ns and the target is slightly decompressed at the later imaging time of 1.5 ns. The laser drive with the 3-ns shaped pulse has a peak intensity of $\sim 1 \times 10^{15}$ W/cm^2 [Fig. 3(d)]. The foot of this pulse (at an intensity of $\sim 5 \times 10^{13}$ W/cm^2) sends a weak shock ($p \approx 7$ Mbar) through the target resulting in a compression of $\rho/\rho_0 \approx 3.4$ at a low adiabat of $\alpha \approx 2$, which is exactly in the region of the current low-adiabat direct-drive ICF design. The main pulse is shaped to launch an adiabatic wave compressing the target to a peak density of ~9 g/cm^3. The target optical depth versus distance is shown at 2.3 ns [Fig. 3(e)] and at 2.9 ns [Fig. 3(f)], measured with an Fe backlighter. The shock is propagating in the target at 2.3 ns, while it just reaches the back side of the target at 2.9 ns.

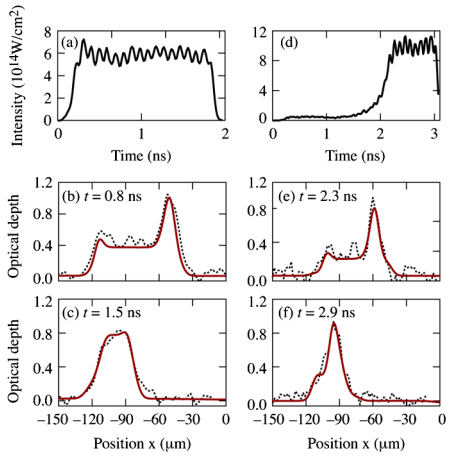

FIG. 3 (color online). (a) The 1.6-ns square laser pulse and the measured (black/dotted curves) and simulated (red/solid curves) optical depth versus target position (along the x axis) at (b) 0.8 ns and (c) 1.5 ns [V backlighter was used]. While panels (d),(e), and (f) represent the case of the 3-ns shaped pulse, and the optical-depth comparison at (e) $t \simeq 2.3$ ns and (f) $t \simeq 2.9$ ns [Fe backlighter was used, respectively.

Figure 4 shows examples of the predicted central density profiles for the 1.6-ns square drive at 0.8 ns [Fig. 4(a)] and 3-ns shaped drive at 2.3 ns [Fig. 4(b)], corresponding to the conditions shown in Figs. 3(b) and 3(e), respectively. It was found that the single shock compresses the target to a peak density of ~4.3 g/cm^3 [Fig. 4(a)], while the low-adiabat compression gives a much higher peak density of ~9 g/cm^3 [Fig. 4(b)]. The experimental density profiles inferred from the measured optical depth are plotted in dash-dotted lines, which show good agreement with the DRACO-predicted ones. The sensitivity of optical-depth measurements allowed density variations of more than ~10%–15% to be measured. As shown in Figs. 3 and 4, the 2D simulations are in good agreement with experimental data for both conditions. The simulations at intermediate times show compression peaks by the main drive (on the right side) and the weak reflected pulse (on the left side). Overall, good agreement has been found for both the peak value of the compression and the target width between experiments and simulations.

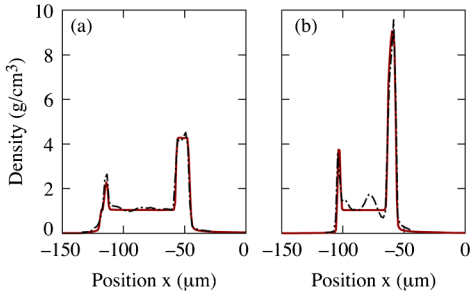

FIG. 4 (color online). The density profiles versus target position from 2D DRACO simulations (solid) and inferred from the measured optical depth (dash-dotted) for the cases of Figs. 3(b) and 3(e), respectively.

The compression at a higher peak intensity of $I \simeq 1.5 \times 10^{15}$ W/cm^2 was performed with 1-ns square pulses. Although such a significantly larger intensity may not be required for direct-drive ICF [3], this experiment was sensitive to the preheat due to hot electrons from two-plasmon-decay (TPD) instability [29,30]. The experimental technique described in this Letter will be used for studying fast-electron preheating in NIF ignition-relevant conditions which may become important at intensities below 1×10^{15} W/cm^2 [31]. Figure 5(a) shows a laser pulse shape (solid curve) and the measured (dashed line) hard x-ray (HXR) signal (with photon energies > 40 keV) using a hard x-ray detector [32]. Hard x rays from hot electrons are produced at the end of the drive starting at 0.6 ns. The measured hot-electron temperature was ~60 keV [33]. Figs. 5(b)–5(d) show the measured target compression at 0.6, 0.9, and 1.1 ns, respectively, for different shots. Data in Figs. 5(b) and 5(c) were obtained with a V backlighter, while Fig. 5(d) was obtained with a Fe backlighter. The Fe backlighter had less attenuation than the V backlighter. It was used to rule out saturation effects of imaging using the V backlighter. While the 2D simulation at 0.6 ns agrees very well with the experiment, there is a significant disagreement at 0.9 and 1.1 ns, when the hard x-ray signal from TPD instability rises.

Simulations including nonlocal heat transport based on a model presented in Ref. [28] were compared with these high-intensity experiments. The nonlocal electrons with energies > 10 keV, from the tail of thermal distribution [28,34–38], can penetrate further into the target and cause more target preheating compared to the local models of energy transport. The nonlocal effects slightly increased the shock velocity in the simulations, but resulted in a

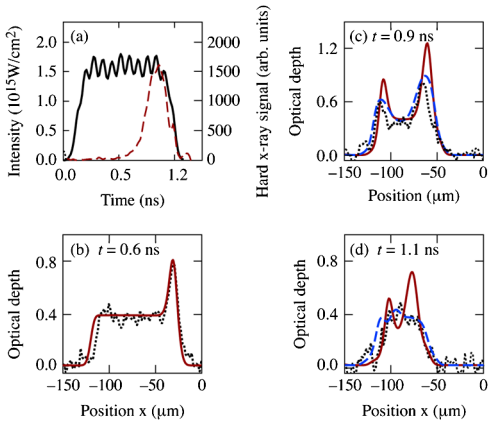

FIG. 5 (color online). (a) The 1-ns pulse shape (solid) and hard x-ray signal (dashed) as a function of time. The optical depth measured (black/dotted), and predicted without preheat (red/solid) and with preheat (dashed/blue) was plotted versus the target position for different shots at (b) $t \simeq 0.6$ ns [V backlighter], (c) $t \simeq 0.9$ ns [V backlighter], and (d) $t \simeq 1.1$ ns [Fe backlighter].

small density reduction of ~10% in the shock-transit stage (before breakout), which cannot explain the observed large decompression at the end of the laser drive.

We have used the astrophysics opacity table (AOT) [39] to postprocess the simulations to obtain the optical depth (OD), which were in good agreement with all experiments except at the later time of high-intensity ($\sim 1.5 \times 10^{15}$ W/cm^2) drives. For the OD discrepancy shown in Figs. 5(c) and 5(d), different opacity models such as PROPACEOS [40] and the average-ion model [41] have been considered. None of the opacity models can consistently give good agreement for both early-time and later-time measurements. This suggests the possibility of fast-electron preheating near the end of such high-intensity drives [42,43].

To model the preheating, hot-electron-energy deposition was included in simulations based on the measured temporal shape of hard x-ray production. Uniform heating of the targets is assumed. The rising temperature due to preheat causes the compressed target to expand so that the density decreases. The simulation results are shown by the dashed blue lines in Figs. 5(c) and 5(d), with a preheat energy ranging from 30 to 40 J. This level of preheating energy is consistent with the observed hard x-ray signal. Once this level of preheating was included, reasonable agreement between simulations and experiments was obtained. Preheating causes the peak density to decrease by almost a factor of 2. In the experiments at lower intensities (shown in Fig. 3), the hot-electron x-ray signal was about 4 times smaller. When included in simulations, this amount of preheat (~ 10 J) did not produce any noticeable density reduction.

In summary, a series of compressibility experiments with ignition-relevant intensities and pulse shapes were performed using planar plastic targets on the OMEGA Laser System. The experiments were simulated using the 2D radiative hydrocode DRACO. For laser intensities less than ~10^{15} W/cm^2, the agreement between experiments and simulations are very good. This justifies the equation-of-state (*SESAME*) and hydrodynamics of the shock wave and adiabatic compression wave predicted by DRACO. These results provide the first experimental evidence for low-entropy, adiabatic compression of plastic shells in the laser intensity regime relevant to direct-drive ICF on NIF. A density reduction has been identified near the end of higher-intensity (1.5×10^{15} W/cm^2) drives. This compression degradation was found to correlate with the measured preheat due to hot electrons (with a temperature of ~60 keV) produced by two-plasmon-decay instability. Mitigation of such fast-electron preheating using thick high-Z-doped plastic ablators is under consideration.

This work was supported by the U.S. Department of Energy (DOE) Office of Inertial Confinement Fusion under Cooperative Agreement No. DE-FC52-08NA28302, the University of Rochester, and the New York State Energy Research and Development Authority.

*shu@lle.rochester.edu
†Also at Nuclear Research Center, Negev, Israel.
‡Also at Department of Mechanical Engineering and Department of Physics & Astronomy, University of Rochester, Rochester, New York 14623-1299, USA.

[1] J. D. Lindl, Phys. Plasmas **2**, 3933 (1995).
[2] S. E. Bodner *et al.*, Phys. Plasmas **7**, 2298 (2000).
[3] S. Atzeni and J. Meyer-ter-Vehn, *The Physics of Inertial Fusion* (Clarendon Press, Oxford, 2004); P. W. McKenty *et al.*, Phys. Plasmas **8**, 2315 (2001).
[4] E. M. Campbell and W. J. Hogan, Plasma Phys. Controlled Fusion **41**, B39 (1999).
[5] S. P. Regan *et al.*, Phys. Plasmas **14**, 056305 (2007).
[6] T. R. Boehly *et al.*, Phys. Rev. Lett. **87**, 145003 (2001).
[7] D. Hoarty *et al.*, Phys. Rev. Lett. **78**, 3322 (1997).
[8] O. L. Landen *et al.*, J. Quant. Spectrosc. Radiat. Transfer **71**, 465 (2001).
[9] G. Gregori *et al.*, J. Quant. Spectrosc. Radiat. Transfer **99**, 225 (2006).
[10] S. H. Glenzer *et al.*, Phys. Rev. Lett. **98**, 065002 (2007).
[11] S. Fujioka *et al.*, Phys. Plasmas **10**, 4784 (2003).
[12] S. Fujioka *et al.*, Rev. Sci. Instrum. **74**, 2198 (2003).
[13] H. Azechi *et al.*, Phys. Rev. Lett. **98**, 045002 (2007).
[14] L. B. Da Silva *et al.*, Phys. Rev. Lett. **78**, 483 (1997).
[15] G. W. Collins *et al.*, Science **281**, 1178 (1998).
[16] A. N. Mostovych *et al.*, Phys. Rev. Lett. **85**, 3870 (2000).
[17] M. D. Knudson *et al.*, Phys. Rev. Lett. **87**, 225501 (2001).
[18] T. R. Boehly *et al.*, Phys. Plasmas **11**, L49 (2004).
[19] D. C. Swift *et al.*, Phys. Plasmas **12**, 056308 (2005).
[20] R. L. McCrory *et al.*, J. Phys. IV (France) **133**, 59 (2006).
[21] T. R. Boehly *et al.*, Opt. Commun. **133**, 495 (1997).
[22] Y. Lin, T. J. Kessler, and G. N. Lawrence, Opt. Lett. **20**, 764 (1995).
[23] T. R. Boehly *et al.*, J. Appl. Phys. **85**, 3444 (1999).
[24] S. P. Regan *et al.*, J. Opt. Soc. Am. B **17**, 1483 (2000).
[25] D. K. Bradley *et al.*, Rev. Sci. Instrum. **63**, 4813 (1992).
[26] R. C. Malone, R. L. McCrory, and R. L. Morse, Phys. Rev. Lett. **34**, 721 (1975).
[27] J. Delettrez, Can. J. Phys. **64**, 932 (1986).
[28] V. N. Goncharov *et al.*, Phys. Plasmas **13**, 012702 (2006).
[29] A. Simon *et al.*, Phys. Fluids **26**, 3107 (1983).
[30] C. Stoeckl *et al.*, Phys. Rev. Lett. **90**, 235002 (2003).
[31] R. L. McCrory *et al.*, Phys. Plasmas (to be published)
[32] C. Stoeckl *et al.*, Rev. Sci. Instrum. **72**, 1197 (2001).
[33] B. Yaakobi *et al.*, Phys. Plasmas **12**, 062703 (2005).
[34] A. R. Bell, R. G. Evans, and D. J. Nicholas, Phys. Rev. Lett. **46**, 243 (1981).
[35] D. Shvarts *et al.*, Phys. Rev. Lett. **47**, 247 (1981).
[36] J. F. Luciani, P. Mora, and J. Virmont, Phys. Rev. Lett. **51**, 1664 (1983).
[37] A. Sunahara *et al.*, Phys. Rev. Lett. **91**, 095003 (2003).
[38] G. Schurtz *et al.*, Phys. Rev. Lett. **98**, 095002 (2007).
[39] W. F. Huebner *et al.*, Los Alamos National Laboratory, Los Alamos, NM, Report LA-6760-M, 1977 (unpublished).
[40] J. J. MacFarlane, I. E. Golovkin, and P. R. Woodruff, J. Quant. Spectrosc. Radiat. Transfer **99**, 381 (2006).
[41] H. Takabe and T. Nishikawa, J. Quant. Spectrosc. Radiat. Transfer **51**, 379 (1994).
[42] W. Seka *et al.*, Phys. Plasmas **15**, 056312 (2008).
[43] V. N. Goncharov *et al.*, Phys. Plasmas **15**, 056310 (2008).